J. R. S. Interface, Supplementary Material: Accumulation of dead cells from contact killing facilitates coexistence in bacterial biofilms

Gabi Steinbach,[1] Cristian Crisan,[2,3,4] Siu Lung Ng,[2,3,4] Brian Hammer,[2,3,4] and Peter Yunker[1]

[1]*School of Physics, Georgia Institute of Technology, Atlanta, GA, USA.*

[2]*School of Biological Sciences, Georgia Institute of Technology, Atlanta, GA, USA.*

[3]*Center for Microbial Dynamics and Infection, Georgia Institute of Technology, Atlanta, GA, USA.*

[4]*Institute for Bioengineering and Biosciences, Georgia Institute of Technology, Atlanta, GA, USA.*

MATERIALS AND METHODS

Bacterial strains

For experiments presented in figures in the main text, we used the *qstR** constitutive killer *V. cholerae* C6706 and derivatives of it (Tab. I). Isogenic mutual killer experiments competed SN441 and JT1052; JT1052 was engineered from C6706 by replacing the aux1 and aux2 clusters with clusters from an environmental *V. cholerae* isolate 692-79 [1]. Experiments with unidirectional killing employed a T6SS-active strain SN441 against a target strain JT1053, which was a T6SS-defective mutant of JT1052, prepared via *vasK* deletion. The SN441 killer strain constitutively expresses a superfolder green fluorescent protein (sfGFP).

Construction of genetically altered *V. cholerae* strains

All *V. cholerae* mutant strains were constructed using allelic exchange methods as described previously [2] and confirmed by PCR and sequencing. Restriction enzymes, polymerases and Gibson assembly mix reagents were used to manipulate DNA fragments and plasmids according to manufacturer instructions (New England Biolabs and Promega).

Sample preparation

All bacterial strains (apart from *V. harveyi*) were grown overnight in lysogeny broth (LB), and then back-diluted in fresh LB for an additional 3h at 37°C. Only *V. harveyi* was grown overnight

TABLE I. **Strain names and specifications.**

Strain	**Genotype**	**Role**	**Ref.**
V. cholerae C6706 (SN441)	Ptac-*qstR*, ΔVC1807::Ptac-*sfGFP*	killer (Fig. 1-3, Fig. 4(b,e,g,i), Fig. S1-S3)	this study
V. cholerae C6706 (SN426)	Ptac-*qstR*, ΔVC1807::Ptac-*sfGFP*, Δ*vasK*	defective killer (Fig. 4(c,f,h,j), Fig. S4)	this study
V. cholerae C6706 (JT1052)	Ptac-*qstR*, Replaced T6SS aux1 and aux2 gene clusters with ones from 692-79	killer (Fig. 3, Fig. S1 (a,b,c))	[1]
V. cholerae C6706 (JT1053)	Ptac-*qstR*, Replaced T6SS aux1 and aux2 gene clusters with ones from 692-79, Δ*vasK*	target (Fig. 1-4, Fig. S1d and Fig. S2)	[1]
V. cholerae 692-79	wild type	killer (Fig. S3 and Fig. S4)	[3–5]
V. cholerae 2631-78	wild type	killer (Fig. S3 and Fig. S4)	[4, 5]
V. cholerae VC56	wild type	killer (Fig. S3 and Fig. S4)	[4–6]
V. cholerae 3223-74	wild type	killer (Fig. S3 and Fig. S4)	[4, 5]
E. cloacae ZOR0014	wild type	killer (Fig. S3 and Fig. S4)	[7, 8]
V. harveyi BB120	wild type	target (Fig. S3)	[9]

at 30°C in marine (LM) medium. For each competition experiment, liquid co-cultures of two strains were mixed, accordingly. For measurements of spatio-temporal dynamics in unidirectional killing (Fig. 1c in main text), we employed four different killer to target volume mixing ratios: 1:1, 1:2, 1:5, and 1:10. (Note that in Fig. 1 (main text), these ratios do not reflect the fraction of killer cells at 0 h. After inoculation, strain fractions were extracted only once a dense monolayer had formed, which then contains altered strain fractions.) For volume mixing ratios in all other experiments, refer to details given in the main text. Liquid cultures were either aliquoted $OD_{600} = 1$ or $OD_{600} = 10$ (see main text for each experiment). To achieve an effective $OD_{600} = 10$, cultures with an $OD_{600} = 1$ were centrifuged and re-suspended 1/10 the volume of fresh medium. After preparation of liquid co-cultures, they were inoculated on agar pads. We prepared 1.5% LB agar pads (1.5% LM agar pads used for *V. harveyi*) and added 7μl of 100μg/ml propidium iodide (PI) on the agar pad surface. After the PI droplet dried, 1μl of liquid co-culture was inoculated on that same spot. For measurements in vertical confinement, a cover glass was placed on top of the agar pad directly after inoculation. All biofilms were grown under optimal conditions in either an Okolab caged incubator attached to the confocal microscope (time-lapse measurements) or a separate incubator box (single-time measurements after 24h of growth). Biofilms were grown at 37°C, but co-cultures containing *V. harveyi* were grown at 30°C.

Microscopy

All images were recorded with a Nikon A1R confocal microscope. We used FITC and TRITC filters for recording the fluorescence signal from the sfGFP expressing cells and the PI-labeled DNA of dead cells. We used bright-field mode for recording bright-field images. The microscope is additionally equipped with an OkoLab incubator box (operated at 37°C and maximum humidity) to ensure optimal growth conditions. Samples in 2D confinement were imaged with a 60X oil immersion objective (NA=1.45) and a vertical step size of 0.5μm. For unconfined growth, images were taken with a 40X long distance objective (NA=0.6) and with a vertical step size of 2μm. For time-lapse recordings of the two-strain coarsening process, images were recorded every 10 minutes. Tracking of PI-labeled single dead cells was performed in 5 minutes sequences.

Image processing and analysis

All image processing and analysis was performed with Fiji. The fraction of the fluorescent strain (main text Fig. 1c, Fig. 4) was extracted from recorded sfGFP signal in microscopy time lapse images. The image series was first adjusted for changes in fluorescence intensity over time using a bleach correction function that was obtained from the intensity change of a reference biofilm which consists of fluorescent cells only. The fraction of the fluorescent strain was then obtained by thresholding the corrected fluorescent images, and counting pixels that contain sfGFP fluorescence intensity above the threshold value. We confirmed that the choice of the threshold value did not impact the identified time when killing halts (Fig. S1 a). For example, in the 1:2 killer to target competition, the killer reached 90 % of its final size after the same time at 3.2 h independent of the threshold value.

To determine the mean relative PI intensity as a function of distance from the interface between strains (Fig. 2 f), first a threshold image obtained from the sfGFP channel was created as described above. Then, the interface lines where identified via an edge detection and a mask was created that covers all area residing within a distance r from the interface lines. The mask was applied to both the fluorescence image containing the PI signal and the bright-field image. We then measured the mean brightness intensity (PI or bright-field signal) within the area covered by the mask. This gives the mean brightness intensity for distance r. The obtained curve of mean brightness intensities as a function of distance was normalized to a range between 0 and 1. We additionally tested the sensitivity of the extracted interface width curves on the threshold value that was applied to

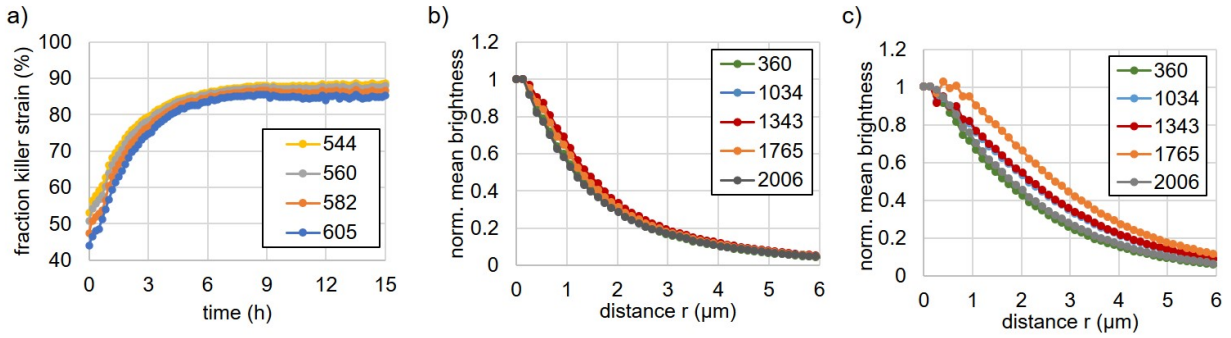

Fig. S1. **Sensitivity of image analysis on the threshold value.** a) The curves show the extracted fraction of killer cells in a phase separating biofilm (inoculated with a 1:2 killer to target ratio) under different threshold values (see legend) for time lapse images with pixel intensities ranging from 71-2935. b) Mean intensity of PI signal and b) mean intensity of inverted bright-field signal within a distance r from the interface between competing strains for different threshold values (see legend) of the masked image, which had pixel intensities ranging from 36-3620.

the sfGFP channel image (Fig. S1 b,c). For a large range of threshold values, the PI brightness reached the half maximum value at a distance from 1.2 μm to 1.4 μm. For bright-field images, the half maximum value is reached between distances from 1.6 μm to 2.6 μm. All values are on the order or larger than a cell length, providing protection against T6SS attack.

To analyze individual dead cells (Fig. 2h), we detected single spots in images from the PI channel and measured the number of detected spots and the mean size per spot (Supplementary Fig. 2) per recorded time point.

The structural analysis of the phase-separation of two competing strains in Fig. 3 was performed via a Fourier transform analysis as described in [3]. In short, we applied a Fourier transformation on the fluorescence image of phase-separating strains. Next, we calculated the structure factor, $S(q)$ by radial integration of the Fourier transformed image. We then determined the characteristic wavenumber, q_m, which is the mean wavenumber q weighted by $S(q)$ as $q_m = \int qS(q)dq / \int S(q)dq$. From this, the characteristic domain length was obtained as $L = \frac{2\pi}{q_m}$, and the mean structure factor, S(L), corresponds to the height of $S(q)$ at q_m.

For the analysis of biofilms grown without confinement (Fig. 4 e-j), we recorded z-stacks that cover the full biofilm thickness and corrected the images for the decrease in fluorescence intensity with increasing biofilm depth. The correction values were obtained from a recorded a z-stack of a biofilm consisting of a single, fluorescent strain, where we normalized the mean fluorescence intensity as a function of biofilm depth. The huge intensity variation across a biofilm of 95μm

thickness required to record the biofilms in two separate sections: high laser power and gain were applied to image the lower section, and low values were applied for intermediate and upper sections. Using the same settings, the co-culture biofilms are imaged and corrected according to the depth dependent intensity variation measured from the single-strain biofilm.

SUPPORTING FIGURES

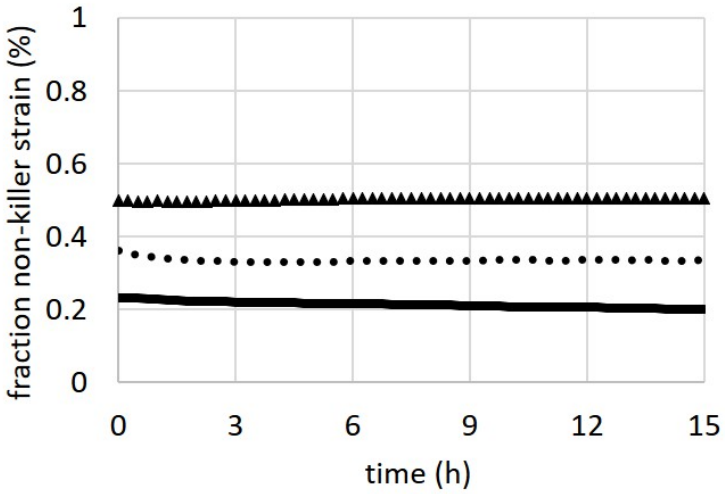

Fig. S2. **Spatio-temporal analysis of confined biofilm growth absent T6SS-mediated killing.** For a biofilm growing from two non-killer strains (one fluorescent and one non-fluorescent), we record time lapse images via confocal microscopy and extract the relative abundance of the fluorescent cells over time for three different initial conditions (fluorescent cell relative abundance during inoculation: 0.5, 0.33, 0.17, from top to bottom curve). In all cases, the fraction of fluorescent cells changes less than 3% of the recorded biofilm area (0.019 mm^2) over the recording time of 15 h.

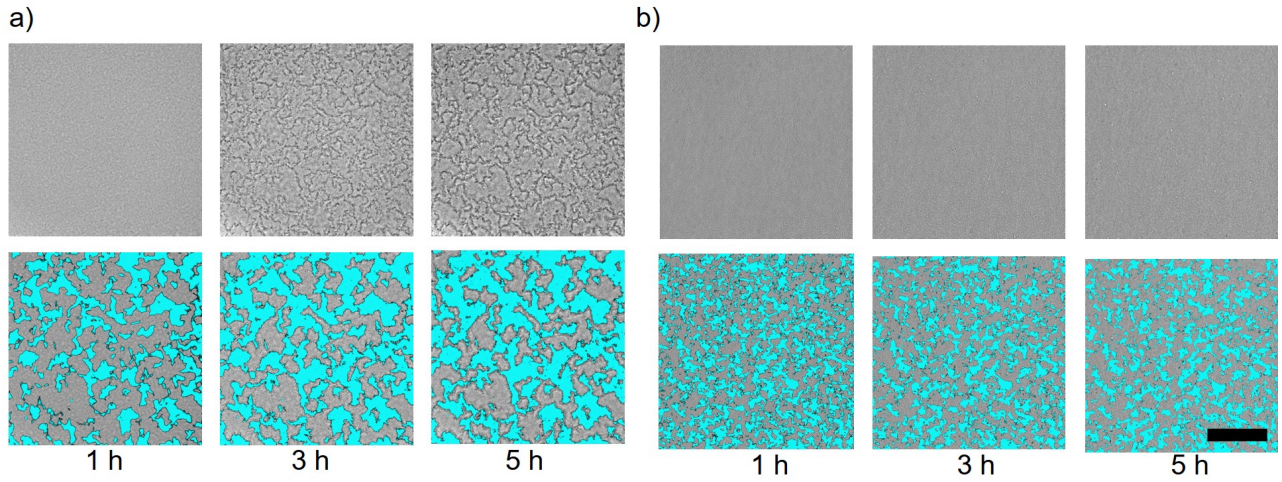

Fig. S3. **Time lapse images of killer and non-killer biofilms** a) Confined biofilms of a killer and target strain, showing brightfield only (top row) and overlaid with fluorescent signal of the killer (bottom row) at 1 h, 3 h, and 5 h. Dark outlines are visible at the strain interface at 3 h, and continue to darken. b) Same as (a) but absent contact killing. Dark outlines are absent at all times. (Scale bar: 50 m)

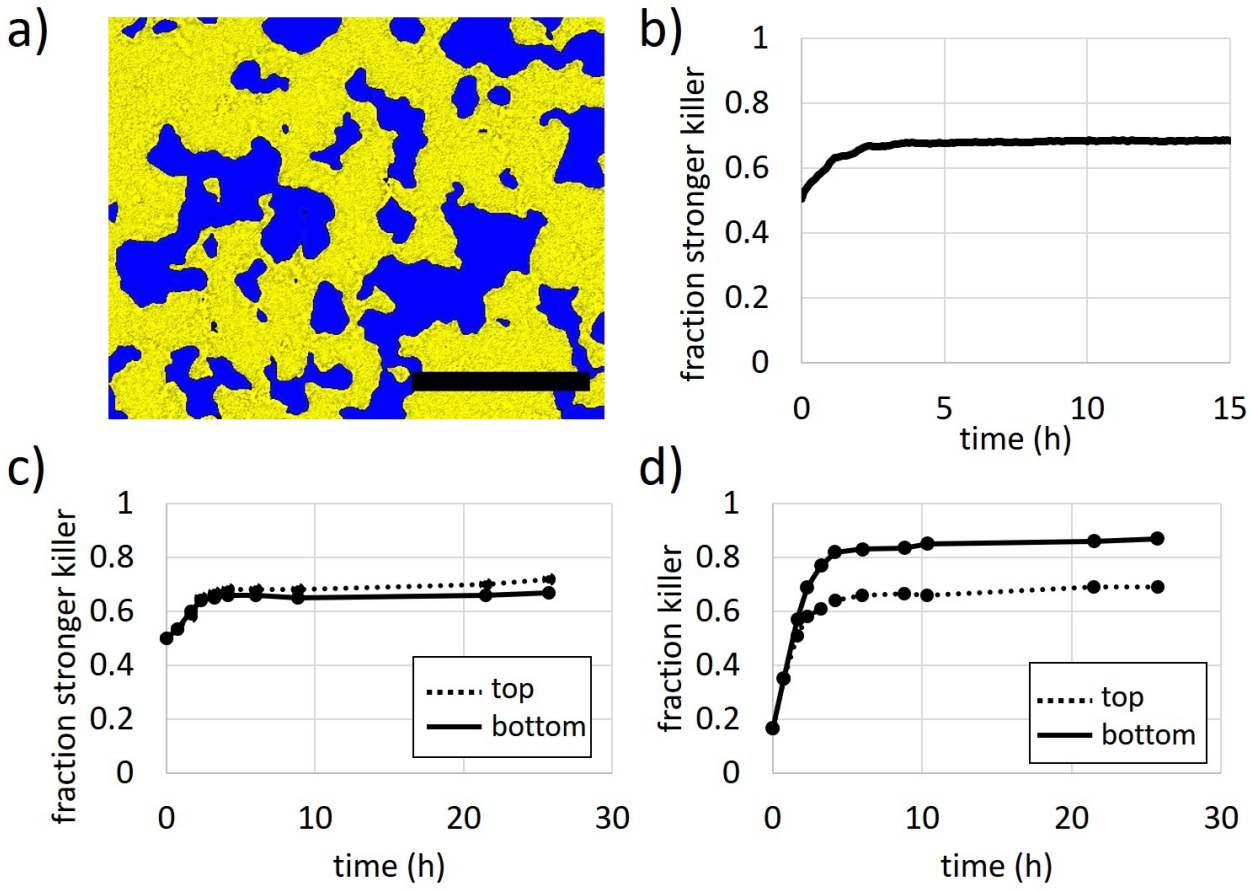

Fig. S4. **Spatio-temporal analysis of phase separation with and without confinement.** a) T6SS-mediated contact killing between mutual killers (initial number ratio of 1:1) leads to the formation of clonal patches (S video) as shown here by a fluorescent microscopy overlaid on a bright field image image. The observed domain formation agrees with previous findings [3]. The image is recorded after 7 h of biofilm growth in 2D confinement. (Scale bar: 50μm) The fraction of the more potent killer increases at early times followed by a significantly slower increase after 3 h in both cases for 2D confinement (b) and without confinement, i.e. without cover glass on top (c), where the latter shows almost identical fractions at the top and the bottom of the biofilm. (d) In the case of unidirectional killing in unconfined growth, we obtain a similar temporal behavior, but here the killer expands more at the bottom of the biofilm than at the top. This is consistent with findings in the main text Fig. 4i.

.

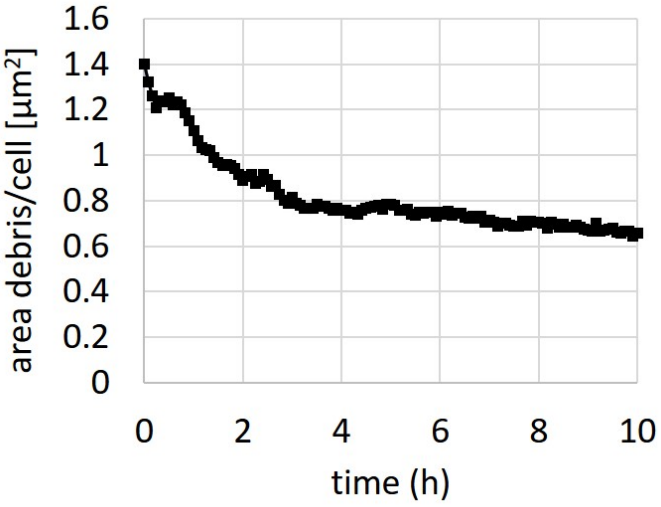

Fig. S 5. **Persistence of dead cell debris.** The PI-labeled area per dead cell is recorded over time by tracking individual dead cells over 10 h and extracting the mean PI-labeled area per dead cell. After a quick decline (due to compression or degradation of cell debris), the amount of labeled area saturates, demonstrating that PI-labeled DNA persists several hours after cell death. The data are obtained from a dense mix of killer and target cells (number ratio of 50:1, inoculated at OD_{600} =10), ensuring that most dead target cells are sufficiently far from each other to enable long-time tracking.

.

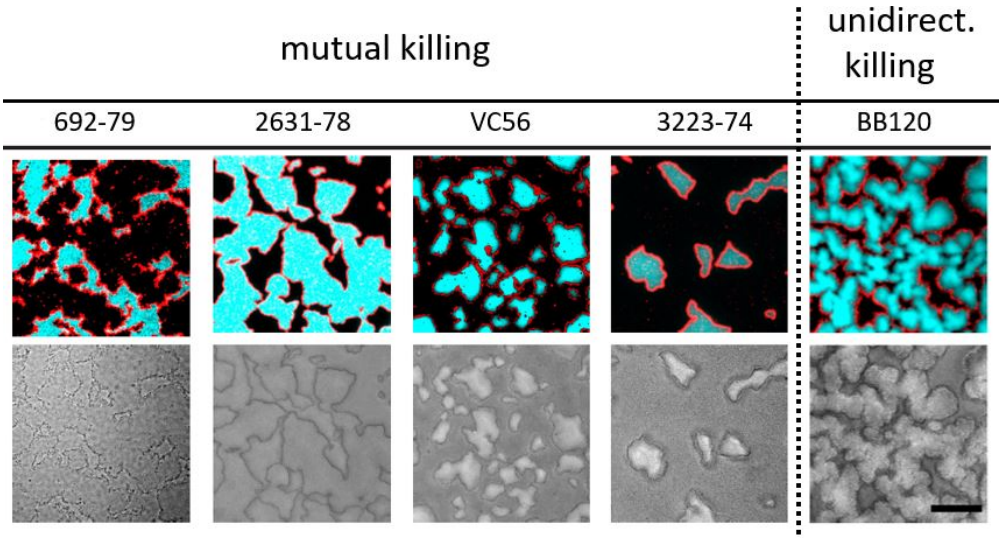

Fig. S6. **Competition outcomes from mutual and unidirectional killing between nonisogenic competitors, involving the C6706 T6SS+ killer strain.** The C6706 T6SS+ killer strain is competed against other T6SS+ killers (mutual killing) and non-killer target strains (unidirectional killing). The top row depicts fluorescent microscopy images containing the fluorescent C6706 killer strain (cyan) and PI-labeled cell debris. The T6SS-proficient competitor strains (four different *V. cholerae* strains) and the non-killer competitor strain *V. harveyi* are not fluorescent and appear black. The bottom row depicts the same areas of view but as brightfield images. For all strain combinations, we observe that PI-labeled dead cell debris accumulates at the interface between competitors, and optical intensity variations occur at the interface between strains in the bright-field images (though please note, non-isogenic strains exhibit different intensities in bright-field imaging, partially, but not completely, obscuring the dark outlines between strains). For each strain combination, the initial number ratio between C6706 and its competitor strain was adjusted (ranging from 1:1 to 1:5) such that large domains of each strain were observed after 24 h of biofilm growth. All co-cultures were incubated at $OD_{600} = 1$. Scale bar: 50μm.

.

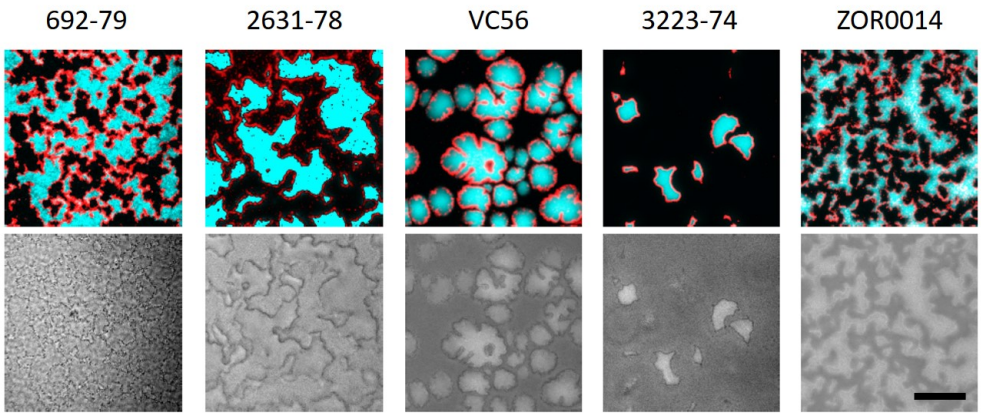

Fig. S 7. **Unidirectional competition outcomes between a T6SS-defective C6706 strain and other, non-isogenic T6SS+ killer strains.** The top row depicts fluorescent microscopy images containing the fluorescent C6706 killer strain (cyan) and PI-labeled cell debris. The T6SS-proficient competitor strains (four different *V. cholerae* strains and *E. cloacae* (data not shown)) are not fluorescent and appear black. The bottom row depicts the same areas of view but as brightfield image. For all strain combinations, we observe that PI-labeled dead cell debris accumulates at the interface between competitors, and optical intensity variations occur at the interface between strains in the bright-field images. Please note, non-isogenic strains exhibit different intensities in bright-field imaging, partially, but not completely, obscuring the dark outlines between strains. This shows that the accumulation of dead cell debris is a general feature of T6SS mediated killing and occurs from a variety of toxins. For each image the initial number ratio between C6706 and its competitor strain was adjusted (ranging from 1:3 to 1:5) such that large domains of each strain were observed after 24 h of biofilm growth. All co-cultures were incubated at $OD_{600} = 1$. Scale bar: 50μm.

SUPPORTING MOVIES

Video 1. **Population dynamics in a biofilm composed of mutually killing *V. cholerae* strains.** Time-lapse images of a vertically confined biofilm composed of T6SS-proficient, mutually killing *V. cholerae* strains recorded with confocal microscopy. The recordings show brightfield images with overlaid fluorescence signal from one killer strain (cyan); the other killer strain is not fluorescent.

Video 2. **Accumulation of dead cell debris in a biofilm composed of mutually killing *V. cholerae* strains.** Time-lapse images of a vertically confined biofilm composed of T6SS-proficient, mutually killing *V. cholerae* strains recorded with confocal microscopy. The recordings show brightfield images with overlaid fluorescence signal from one killer strain (cyan); the other

killer strain is not fluorescent. Dead cell debris appears red from PI labeling.

Video 3. **Mechanical perturbation in a biofilm with unidirectional killing.** Time-lapse images of a vertically confined, growing *V. cholerae* population composed of a T6SS+ killer strain and a T6SS- target strain recorded with confocal microscopy. The recordings show brightfield images with overlaid fluorescence signal from the killer strain (cyan); the target strain is not fluorescent. The time, given in hours, gives negative values for the period before a dense biofilm has formed. Positive values count the time after dense packing of cells has been obtained.

REFERENCES

[1] J. Thomas, S. S. Watve, W. C. Ratcliff, and B. K. Hammer, mBio **8**, e00654 (2017).

[2] K. Skorupski and R. K. Taylor, Gene **169**, 47 (1996).

[3] L. McNally, E. Bernardy, J. Thomas, A. Kalziqi, J. Pentz, S. P. Brown, B. K. Hammer, P. J. Yunker, and W. C. Ratcliff, Nat Commun. **8**, 14371 (2017).

[4] E. E. Bernardy, M. A. Turnsek, S. K. Wilson, C. L. Tarr, and B. K. Hammer, Appl Environ Microbiol. **82**, 2833 (2016).

[5] S. S. Watve, A. T. Chande, L. Rishishwar, L. Mario-Ramrez, I. K. Jordan, and B. K. Hammer, Genome Announc. **4**, e01396 (2016).

[6] C. V. Crisan, A. T. Chande, K. Williams, V. Raghuram, L. Rishishwar, G. Steinbach, S. S. Watve, P. Yunker, I. K. Jordan, and B. K. Hammer, Genome Biol. **20**, 163 (2019).

[7] W. Z. Stephens, A. R. Burns, K. Stagaman, S. Wong, J. F. Rawls, K. Guillemin, and B. J. M. Bohannan, ISME J. **10**, 644 (2016).

[8] B. H. Schlomann, T. J. Wiles, E. S. Wall, K. Guillemin, and R. Parthasarathy, Proc Natl Acad Sci USA. **116**, 21392 (2019).

[9] B. L. Bassler, E. P. Greenberg, and A. M. Stevens, J Bacteriol. **179**, 4043 (1997).